OXFORD

Journal of Geophysics and Engineering

Journal of Geophysics and Engineering (2022) **19**, 1–13 https://doi.org/10.1093/jge/gxab067

Velocity gradients choice affecting seismic site response in deep alluvial basins: Application to the Venetian Plain (Northern Italy)

Valeria Cascone*, Ilaria Barone and Jacopo Boaga

Geoscience Department, University of Padova, Via G. Gradenigo 6, Padova, 35131, Padova, Italy

*Corresponding author: Valeria Cascone. E-mail: valeria.cascone@phd.unipd.it

Received 15 December 2020, revised 10 September 2021
Accepted for publication 1 November 2021

Abstract

The average shear-wave velocity of the first 30 metres of subsoil and the depth of the engineering bedrock are considered the key parameters for simplified seismic site response modelling. However, a reliable estimate of the site amplification should consider the entire shear-wave velocity profile from the ground surface down to the engineering bedrock. In deep alluvial basins, a typical geological context where the soil–bedrock interface may lie below the penetration depth of most common prospecting methods, only the shallow velocity profile can be defined in detail, while the deeper structures are commonly extrapolated with linear equations. The choice of a realistic interpolation between the shallow and deep soil still remains an open issue. We compute the 1D seismic site response of two sectors of the Venetian Plain (Northern Italy) characterised by gravelly and sandy deep formations. We model the 1D soil columns using theoretical non-linear gradients proposed in literature for deep alluvial basins. The numerical modelling results, in terms of strong motion parameters, show variations in the seismic site response up to 20%. The effect of the velocity gradients is also evaluated comparing the numerical simulations with real accelerometers recorded by a deep borehole seismometer and a seismic station located at the top of the borehole. These results demonstrate that the selection of the velocity gradient is crucial for seismic site characterisation of deep alluvial basins. In particular, the study suggests which is the most conservative gradient among the ones tested in terms of ground motion hazard estimation.

Keywords: seismic site response, deep alluvial basins, shear-wave velocity, velocity gradients

1. Introduction

The effects of local geology on seismic ground motion have been widely studied in geotechnical earthquake engineering to estimate response spectra for building restoration and construction (Kramer 1996). The shear-wave velocity (V_s) is one of the key parameters adopted for site classification in several seismic regulations (Boore *et al.* 1993, Martin & Dobry 1994). V_s profiles estimate the rigidity of the soil column when excited by seismic shear stress, which is the most important action controlling the seismic site response (Martin & Dobry 1994). Seismic site amplification can be in fact described as the motion modification due to the soft soil during the wave propagation through the stratigraphic column, from the basement bedrock upwards to the ground surface (Langston 2003; Chong & Ni 2009; Rathje *et al.* 2010). Several seismic regulations propose different approaches to evaluate the seismic amplification due to the soil properties. The soils are often classified into different categories, based on the average V_s of the top 30 m of a

soil profile (also called V_{s30}) as in the Italian Building Code ('Norme tecniche per le costruzioni–NTC'; Ministero delle Infrastrutture e dei Trasporti 2008); or the Eurocode 8–EC8 (European Committee for Standardisation 2004); and the National Earthquake Hazard Reduction Program-NEHRP provisions (Building Seismic Safety Council–BSSC 2003).

The V_{S30} parameter adopted by the seismic site classification considers the first 30 metres of subsoil, which is the depth of investigation for common geophysical and geotechnical analysis, that are logistically and economically often limited to the first subsoil. Seismic surveys to retrieve V_S values can be made either in boreholes (down-hole seismic testing, Cardarelli *et al.* 2018) or with surface methods as the multichannel analysis of surface waves (MASW, Park *et al.* 2000; Strobbia *et al.* 2011) and SH refraction analysis, (Hunter *et al.* 2002). Regardless of the method adopted in common engineering projects, the investigation depth rarely exceeds the first subsoil, being limited by the logistically achievable efforts such as: seismic source power, extension of the survey length due to urban conditions, borehole penetration etc. Thus, most of the seismic site response studies are based on the properties of the subsurface soils down to 30 metres (Boore *et al.* 1993; Martin & Dobry 1994).

The Italian and European seismic codes define the engineering bedrock as the depth at which $V_S \geq 800$ m s^{-1} (soil category A = stiff soil or rock, see EC8). Softer soils, with $V_S \leq 800$ m s^{-1}, are expected to amplify the seismic action, therefore the correct estimation of the site amplification should consider the entire soil profile from the ground surface down to the engineering bedrock. Nevertheless, in deep alluvial basins, a clear soft soil–bedrock interface may not be evident but buried under hundreds of metres of soft sediments (Guèguen *et al.* 2007; Poggi *et al.* 2012; Faccioli *et al.* 2015; Mascandola *et al.* 2019). In these geological contexts, thick and soft sediments are expected to amplify the seismic ground motion (Kramer 1996). The site classifications that consider only the V_{S30} might lack a correct seismic action estimation, leading to inaccurate evaluations of the ground amplification level (e.g. Borcherdt 1994; Pitilakis *et al.* 2006). Several available techniques, such as passive surveys and travel-time seismic tomography allow a deeper soil characterisation, down to hundreds of metres deep. The passive methods, based on the recording of ambient vibrations, use 2D arrays of receivers (e.g. SPAC, Aki 1957; frequency–wavenumber method, Lacoss *et al.* 1969), linear arrays (Re-Mi, Louie 2001; Strobbia *et al.* 2015) or single station measurements (HVSR, Nakamura 1989). Passive methods are powerful and cost effective, but they could suffer from a non-uniform distribution of noise sources and can be biased by 2D site effects (Claprood & Asten 2010). Travel-time tomography use signals from earthquakes or low-frequency seismic ambient noise to retrieve deep geological structures. Barbellini *et al.* (2017) propose that the reference bedrock depth of deep alluvial basins could be extrapolated using regional models inferred from travel-time seismic tomography. However, since tomographic approaches are orientated to large scale modelling, retrieved models are sufficiently accurate at depth (i.e. at the kilometric scale), but they often do not present enough resolution for local-scale seismic waveform studies, as needed for local hazard assessment and evaluation of earthquake scenarios.

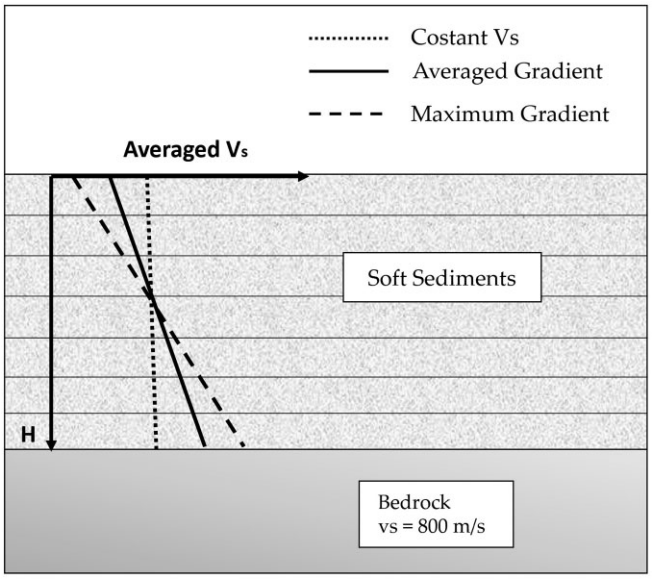

Figure 1. Extrapolation of V_S profiles with linear gradients suggested by the Italian Seismic Code (ICMS 2018, modified).

As matter of fact, the V_S profile characterising the soil column may be accurate for the first tens of metres, thanks to local geophysical/geotechnical surveys, and at few kilometres deep if regional tomographic models are available. However, the velocity structure between the uppermost velocities (e.g. Vs_{30}) and the engineering bedrock ($V_S \geq 800$ m s^{-1}) may be not accurately defined, especially in deep alluvial basins. The most adopted ground motion modelling approaches, such as the 1D seismic site response, need the complete characterisation of the soil column, at least until the reference engineering bedrock depth. For these reasons, several seismic codes propose simplified approaches to describe the soil column. The Italian Seismic Code (ICMS 2018), for example, proposes an extrapolation of V_S in depth through linear gradients with different slopes (depending on the geological site conditions) until the depth of the engineering bedrock depth (figure 1).

It is known that the seismic motion can be decomposed in different sets of waves such as body waves (P, SH, SV) or surface waves (Rayleigh, Love), and seismic motion amplification may be different. However, it is common practice in earthquake engineering design norms focusing of the effect of near-surface geology for vertically propagating shear body waves (see Eurocode 8, European Committee for Standardisation 2004).

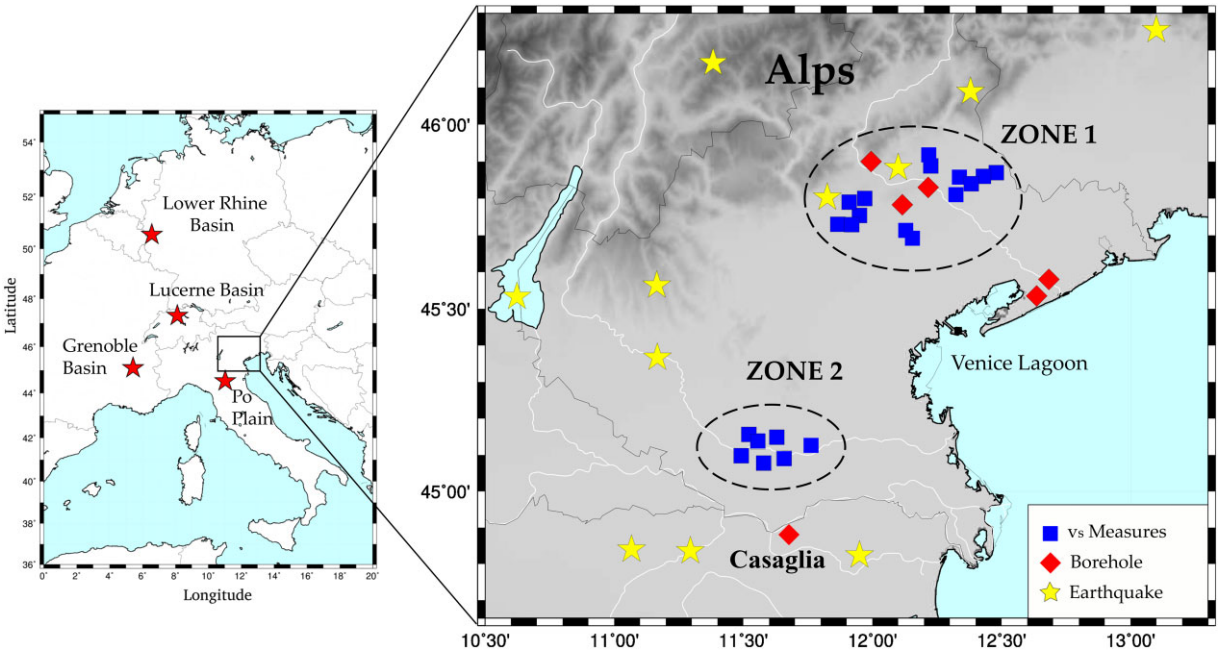

Figure 2. Left panel: Europe chart and deep alluvial basins' locations (red stars): Lower Rhine Basin (Germany); Lucerne Basin (Switzerland); Grenoble Basin (France) and the Po Plain (Italy). Right panel: zoom of Venetian Plain (Italy). Blue squares represent in situ measurement locations. Red diamonds represent ENI/AGIP deep boreholes. Yellow stars indicate the epicentre of the main seismic events from 1117 to 2012 ($5.5 > Mw > 6.8$).

In this study, we perform several 1D seismic site analysis in the Venetian Plain area (Northern Italy), a large and deep sedimentary basin (figure 2). In particular, we consider two different sectors where a detailed set of seismic surveys were performed to obtain shallow V_S profiles, while the deeper structures remain un-investigated. To fill the gap between the shallow and deeper V_S structures, we adopt general gradients, proposed for the modelling of several alluvial basins as the Lower Rhine Basin (Germany; Budny 1984), the Grenoble Basin (France; Guèguen *et al.* 2007) and the Lucerne Basin (Switzerland; Poggi *et al.* 2012). These sites (red stars in figure 2) are in fact characterised by deep sedimentary covers, similarly to the Venetian Plain.

To compare modelling and experimental data we analysed real seismograms coming from a borehole in the Po Plain, where deep and surface seismic recording stations were available. 1D seismic site response modelling was compared to the recording amplifications, testing different gradients.

We aim to assess how the choice of gradient can modify the seismic site response in deep sedimentary basins, where no information about the deeper structures is available. A realistic modelling of the ground motion is the key parameter for ground shaking scenario, used by civil engineers for the design of earthquake-resistant constructions. Due to the limited knowledge of the deeper velocity structures, it could be more appropriate to model the soil column with the gradient which enables the most conservative results in terms of ground motion effects. This study demonstrates the importance of the V_S gradient on ground motion scenarios and the results are relevant for seismic hazard evaluation in deep sedimentary basins, which host large urban environments around the world.

2. Study area: the Venetian Plain

Our study area is the Venetian Plain region (Northern Italy), a large syntectonic alluvial basin actively affected by earthquake occurrence (figure 2). Together with the Po Plain, the Venetian Plain represents the foreland of the S-verging central-southern Alps and the N-NE-verging northern Apennine belt (Doglioni 1993). The effect of the north-propagating Apennine foredeep started in the late Miocene affecting the southern sectors of the Venetian Plain and led to a regional southward tilting recorded up to Venice Lagoon. The thickness of Quaternary formations varies from 2 km in the southern part of the Venice Lagoon, and gradually pinches out eastward (Carminati *et al.* 2003). The buried active fronts of Northern Apennines and Southern Alps are considered seismic sources capable of destructive earthquakes (Poli *et al.* 2008). The epicentre distribution of historical and instrumental earthquakes is shown in figure 2. Although the seismicity is concentrated along the foothills area of the Southern Alps and the Northern Apennines, it is widely recognised that the Venetian Plain is influenced by strong seismic site effects (Vuan *et al.* 2011).

The 3D structural models of the Venetian Plain are principally based on old geophysical information from oil explorations (Doglioni 1993). They are also based on the

TRANSALP (TRANSALP Working Group 2002), a deep seismic reflection measurement collected in the Eastern Alps (Cassinis 2006).

In this study, we consider two different sectors of the Venetian Plain with different Quaternary sedimentary fillings: the 'high' (Northern) and 'low' (Southern) plain, where several shallow V_S measurements were performed (figure 2). The high plain or pre-Alpine zone, here called ZONE 1, has a fluvial and glacial origin and is principally composed of gravel (Carraro *et al.* 2015). The low plain, hereafter ZONE 2, extends from the gravel deposits transition to the Adriatic coast; the subsoil is composed mainly of silt and clay layers with intercalations of sandy layers (Carraro *et al.* 2015).

3. Method

In this work, we simulate the 1D seismic site response of two sectors of the Venetian Plain: the ZONE 1, representing the pre-Alpine sector of the alluvial plain characterised by coarse deposits; the ZONE 2, representing the alluvial plain sector with sandy-clay formations (figure 2). We analyse different sedimentary deposits with a wide granulometry range, which cover an important breadth of different soil types.

In seismic engineering practice, the deep alluvial basin environments are usually represented with 1D geometry of horizontal layering, allowing 1D seismic analysis. With STRATA software (Kottke & Rathje 2009), it is possible to perform stochastic seismic site response analysis with the equivalent-linear approach (Kramer 1996), assuming horizontal soil layer boundaries with an infinite lateral extension and vertically propagating horizontally polarised shear waves (SH waves).

In particular, STRATA code needs: (i) input motions (acceleration time histories); and (ii) soil properties down to the engineering bedrock: the V_S profiles, shear-modulus (G) and damping ratio (D) non-linear curves (Schnabel *et al.* 1972; Idriss & Sun 1992; Boaga *et al.* 2012, 2013), and total unit weight.

In section 4 we illustrate numerical simulations based on the effects of the different type of gradients on 1D seismic analysis. In section 5 we compare the results of a 1D seismic site response with different gradients and real data collected in the Casaglia site (figure 2). In this site, a borehole equipped with two broadband seismometers (a deep and a surface stations) was available (Pesaresi *et al.* 2014).

4. Numerical simulations

4.1. *Input motions*

The seismic site response analysis requires the definition of seismic input terms of acceleration time series. The waveforms can be previously recorded accelerograms belonging to a seismic database, such as the European Strong Motion Database. We select a target response spectrum considering the local probabilistic seismic hazard analysis of the Veneto Region (Northern Italy). We adopt an average expected acceleration of 0.13 *g* with 10% of probability of non-exceedance in 50 years for a return period of 475 years (Italian Seismic Hazard Map, Gruppo di Mappa di Pericolosità Sismica [GdL MPS] 2004) (figure 3a). We use the Rexel program (Iervolino *et al.* 2009) to select a set of one-component real accelerograms. The research criteria consist of an upper and lower tolerance, with respect to the target spectrum, of 30 and 10%, respectively, in a time range between 0.15 and 2 seconds. Three accelerograms are finally selected for our simulation (figure 3b).

4.2. *Definition of V_S profiles*

We model the soil columns combining a detailed shallow V_S profile (down to 30 m) obtained through geophysical surveys and V_S gradients proposed in literature to model deeper layers in alluvial basins. These gradients are adopted when no information is available and an extrapolation until the bedrock depth is required.

4.2.1. Shallow V_S profiles. To characterise the two sites of the Venetian Plain (ZONE 1 and ZONE 2), some geophysical testing campaigns were carried out, including 31 MASW and 36 Re.Mi. surveys. In figure 2 the blue squares represent the locations of the geophysical measurements. The resulting 67 V_S profiles, down to 30 m, are plotted in figure 4. From the plot, it is possible to clearly distinguish between the higher V_S formations in ZONE 1, characterised by coarse sediments, and the lower V_S in ZONE 2 where sand formations are prevalent. The different granulometric distribution of the two study sectors are also confirmed by a deep exploration boreholes log, close to the geophysical measurement locations (red diamonds in figure 2), available on the ViDEPI website (videpi.com). The average V_S profiles for the ZONE 1 and the ZONE 2, marked by red lines in figure 4, match with the velocity structure proposed in the Eurocode 8 (European Committee for Standardisation 2004) for gravelly and sandy soils, respectively. The averaged V_S profiles enable construction of the first 30 m of the 1D soil columns representatives of the two sectors of the Venetian Plain.

4.2.2. Deep Vs profiles. We model the deeper layers (below 30 m until the engineering bedrock) of the 1D soil columns with V_S gradients found in literature. The velocity gradients used in this study are meant to be used for generic deep alluvial basins, characterised by an average sedimentary cover that, in terms of seismic velocity, is similar to the shallow geological formations of the Venetian Plain. Seven different gradients are selected that we will refer to as: EXP (Exponential); PAR (Parabolic); SQR (square root trend); LIN

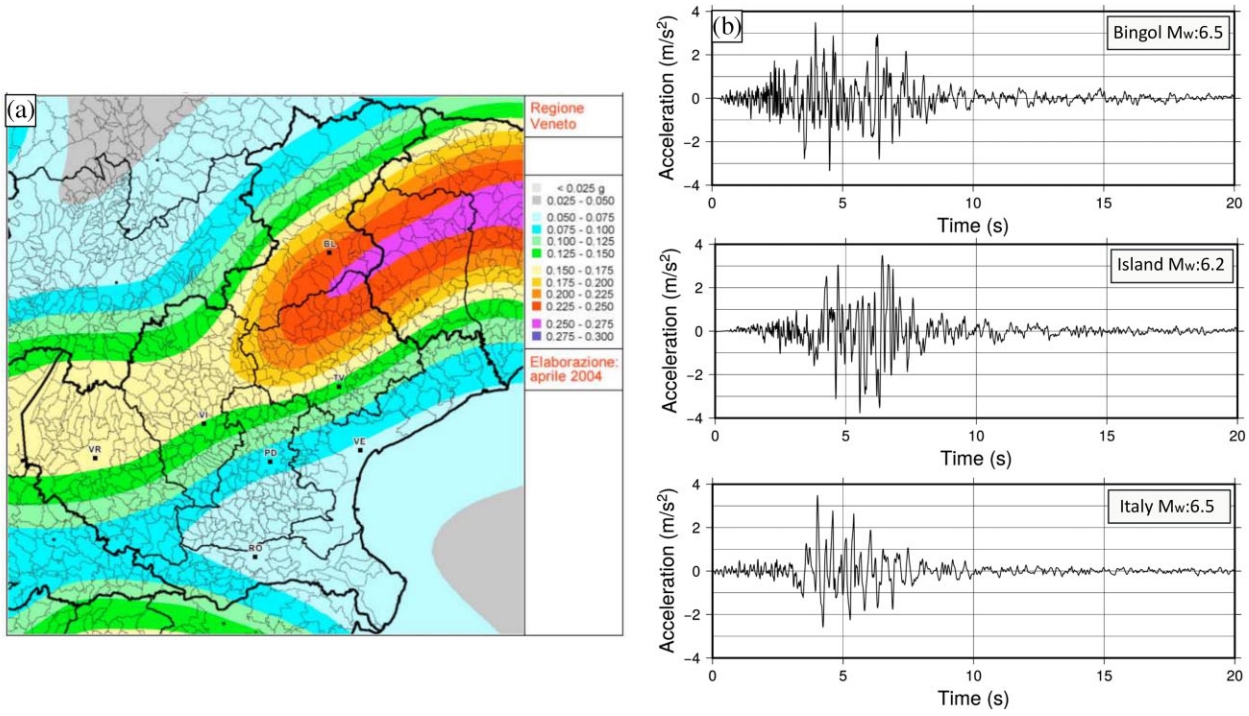

Figure 3. (a) Seismic hazard map of Veneto region, Italy (Italian Seismic Hazard Map, Gruppo di Mappa di Pericolosità Sismica (GdL MPS) 2004, modified). (b) The three-real selected accelerograms used as input motion in our stochastic 1D seismic site response simulations.

(linear); GEN1 and GEN2, (Generics) and HYP, (Hyperbolic). The adopted gradients can be subdivided in two categories. Gradients that do not include the bedrock depth parameter to model the V_S profile (EXP, PAR, SQR) fall into the first category. These gradients make it possible to define the engineering bedrock at different depths, depending on the selected gradient shape. Gradients that include the a priori information of the bedrock depth (LIN, GEN1, GEN2, HYP) belong to the second category.

Considering the geological context of the Venetian Plain, there is no evidence in the literature of the bedrock depth in ZONE 1, while the ZONE 2 was recently investigated by Mascandola *et al.* (2019), who mapped the engineering bedrock of the Po Plain that represents the southern propagation of the Venetian Plain (figure 2). On the basis of the available information, we can model the soil columns of the ZONE 1 with gradients belonging to the first category, while the ZONE 2 is modelled with gradients belonging to the second category, fixing the engineering bedrock at 400 m deep (Mascandola *et al.* 2019).

The theoretical gradients used in this study are described next. In equation (1), the v_0 parameter represents the V_S at the ground surface ($z = 0$).

EXP: Exponential gradient defined as:

$$V_s(z) = V_0(1+z)^x, \quad (1)$$

where x is an exponential coefficient controlling the dependence of velocity with the depth z ($0 < x < 1$). This equation holds for granular media only. Saturation level, fluid pressure and cementation can affect the exponent x (Albarello *et al.* 2011). This is the most common form of the V_S gradients, used to model tectonic basins such as Lower Rhine Basin (Germany) (Budny 1984). In particular, to better define the parameter x for ZONE 1, we use the value found by Budny (1984) for coarse sedimentary cover, equal to 0.285 (yellow curve in figure 5a)

PAR: Parabolic gradient defined as:

$$V_s(z) = V_0\,\sigma_{v0}^{p}, \quad (2)$$

where σ_{v0} represents the total vertical overburden stress (considering a constant value of the soil unit weight) and p is a model parameter, generally varying between 0.1 and 0.3 (Andreotti *et al.* 2018). Equation (2) allows the modelling of a parabolic profile of V_S and is proposed for sedimentary basins by Santamarina *et al.* (2001). To link this curve to the shallow profile we set $\sigma_{v0} = 20\ \mathrm{kN/m^3}$, which is the total unit weight adopted for the 1D soil columns analysed in this study. The p parameter is set to 0.15 (reference value as suggested by Andreotti *et al.* 2018; red curve in figure 5a).

SQR: V_S as a function of the square root of the depth, in the equation:

$$V_s(z) = V_0 + \alpha\sqrt{z}, \quad (3)$$

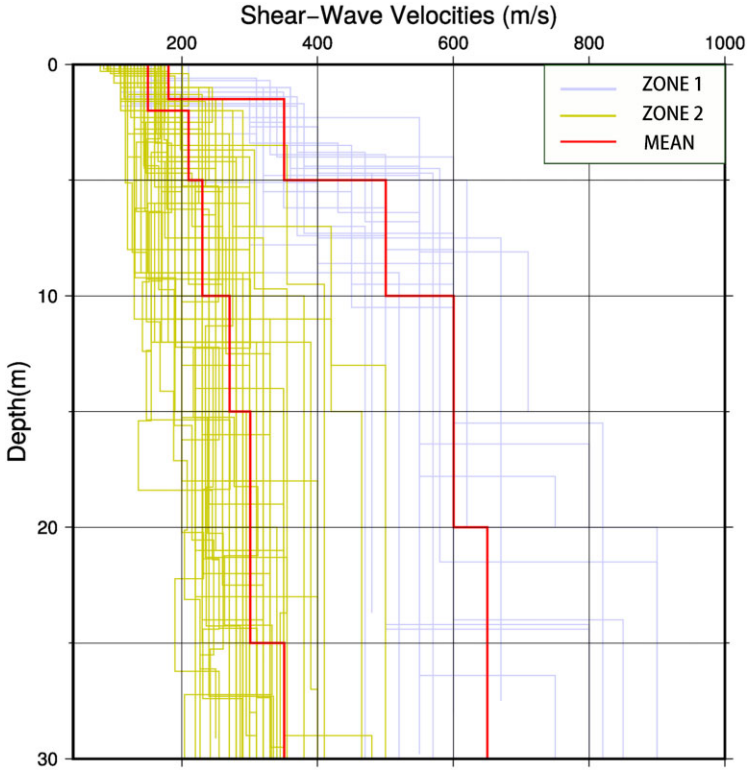

Figure 4. The 67 V_S profiles inferred from geophysical measurements in ZONE 1 (yellow) and ZONE 2 (blue). The red lines represent the mean V_S profiles for the two zones, representative of the shallow part (0–30 m) of the soil columns.

where α is a constant (Guèguen *et al.* 2007). This gradient is considered as a polynomial variation with depth. This equation represents a benchmark basin velocity model inferred from borehole data in Grenoble Basin (France), an Alpine basin with a maximum depth of more than 1 km. It is characterised by a Quaternary infill of coarse glacial deposits, which in terms of velocity is similar to the sedimentary cover of the high Venetian Plain. In our model, we set α equal to 19, which is a reference value taken from Guèguen *et al.* 2007 (purple curve in figure 5a).

LIN: Linear gradient, defined as

$$V_s(z) = mz + q. \tag{4}$$

This is the easiest interpolation between the shallow subsoil ($V_{S\,min}$) and bedrock ($V_{S\,max} = 800$ m s^{-1}). This simplified approach is currently suggested by the Italian Seismic Code (2018) (figure 1). We obtain the linear coefficients with a simple interpolation between the average shear-wave velocity at 30 m deep ($V_{S\,min} = 350$ m s^{-1}) and the bedrock velocity at 400 m deep. This results in a slope of $m = 1.21$ and an intercept of $q = 313.51$ m s^{-1} (dashed red line in figure 5b).

GEN1: The velocity gradient proposed by Régnier *et al.* (2016)

$$V_s(z) = V_{s\,min} + (V_{s\,max} - V_{s\,min}) \left(\frac{z - z_0}{z_2 - z_0} \right)^a. \tag{5}$$

This gradient is used to model simple soil conditions, where V_S increase regularly with depth. $V_{S\,min}$ and $V_{S\,max}$ are the expected minimum and maximum shear-wave velocities, z_0 is the depth of the shallower low velocity layer and z_2 is the bedrock depth. The parameter a is an exponent set equal to 0.25, a reference value taken from Régnier *et al.* (2016). In our model, z_0 is equal to 30 m, z_2 is equal to 400 m; $V_{S\,min}$ and $V_{S\,max}$ are equal to 350 and 800 m s^{-1}, respectively (dashed yellow curve in figure 5b).

GEN2: Generic V_S gradient

This relationship was proposed by Poggi *et al.* (2012) for aseismic characterisation of the Alpine environment in Lucerne Basin (Switzerland). The gradient equation is

$$V_s(z) = (V_{s\,max} - V_{s\,min}) \left[1 - a^{\frac{z_0 - z}{b}} \right] + V_{s\,min}. \tag{6}$$

This equation, similar to GEN 1, adopts curvature coefficients, a and b, which in our model are set to 2.3 and 81.7, so that the basement is reached at 400 m depth (dashed purple curve in figure 5b).

HYP: Hyperbolic profile

This gradient represents the second Gibson model (Gibson 1967). The proposed gradient equation is

$$V_s(z) = V_0 \sqrt{\frac{z_2}{z_2 - z}}, \tag{7}$$

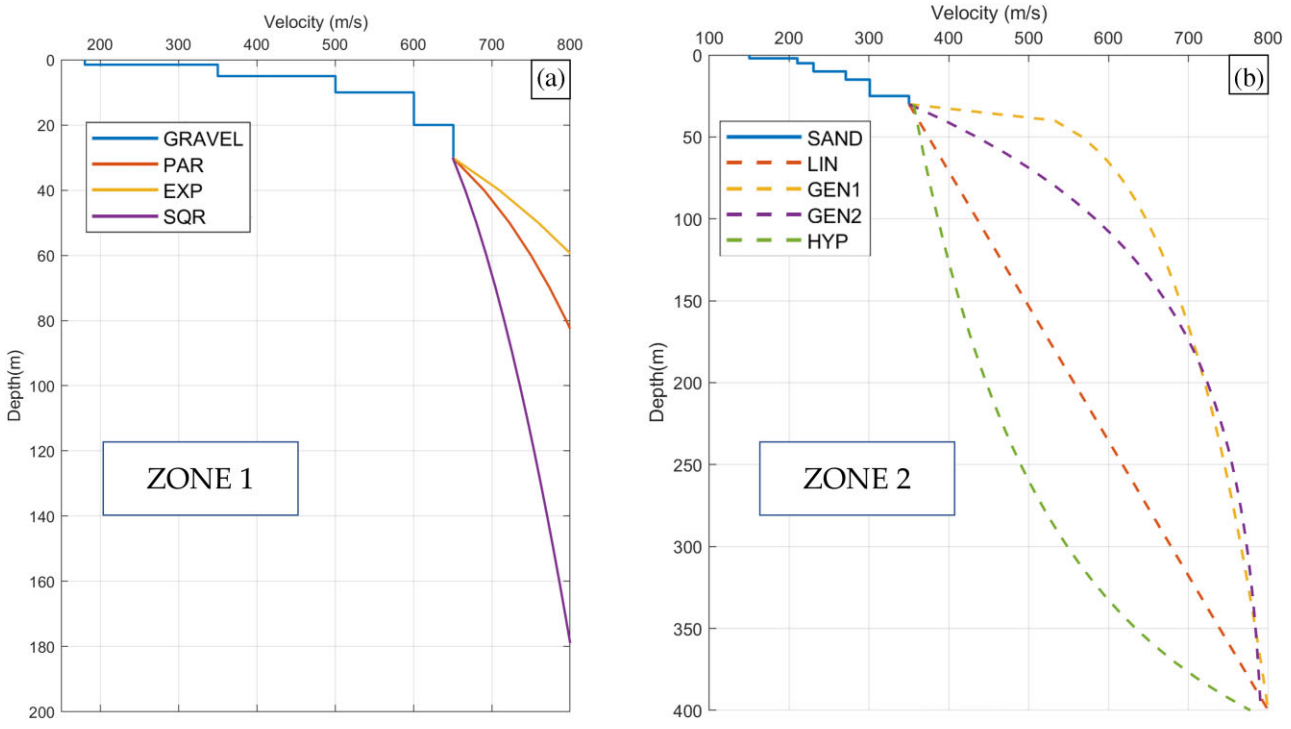

Figure 5. Velocity models adopted for 1D seismic site response for (a) ZONE 1 (case with unknown bedrock depth) and (b) ZONE 2 (case with bedrock depth $z_2 = 400$ m).

where z_2 is the bedrock depth (in our case $v_0 = 350$ m s^{-1} and $z_2 = 400$ m) (dashed green curve in figure 5b).

4.3. *Stochastic 1D seismic analysis*

The entire 1D soil columns with discretised layers are defined to compute the seismic site analysis. We analyse the different velocity profiles shown in figure 5a,b. The shallow layers correspond to the average V_S profiles as indicated in figure 4, while the deeper layers are obtained by discretising the V_S gradient curves with 10-m thick intervals.

The non-linear soil properties are generally represented with a shear-modulus reduction (G/G_{max} V_S shear strain) and damping ratio (D V_S shear strain) curves. In our case, the subsoil is modelled using the modulus reduction and damping curves as proposed by Idriss (1991) for gravel with a total unit weight of 20 kN/m^3 for the soil column of ZONE 1 (solid curves in figure 6a,b). The soil profile characterising the ZONE 2 is modelled with the non-linear curves as proposed by Seed *et al.* (1986) for sandy silt with a total unit weight of 19 kN/m^3 (dashed curves in figure 6a,b).

Once the stratigraphic models are defined, a stochastic analysis via Monte Carlo simulation is performed to consider the local variability. The method consists of an iterative calculation of a deterministic model defined with a set of random realisations. The input parameters are randomly generated on the basis of previously defined probability distributions. In this way, it is possible to simulate the sampling process of a real population to consider the uncertainty of the measurements. In our study, we randomize only the shallow V_S profile in the first 30 m, considering the standard deviation inferred from the statistical distribution of the 67 V_S profiles obtained by *in situ* measurements (figure 4).

The variability of the shallow soil profiles adopted for the stochastic analysis is displayed in figure 7 parts a,b, which illustrate 100 V_S profiles randomly generated. During the simulations, the set of accelerograms described previously (shown in figure 3b) are used as the inputs at the bottom of each soil column. Thus, we perform 300 Monte Carlo simulations for each soil column (100 realisations for each of the three acceleration time histories), for a total of 2100 simulations.

4.4. *Results*

The results, derived from the stochastic 1D seismic site response analysis through Monte Carlo simulations, are presented in terms of surface acceleration response spectra (with a damping ratio, ξ, of 5%), peak ground accelerations (PGA) and Housner Spectrum Intensity (Housner 1952). This last parameter is defined as

$$S_I(\xi) = \int_{0.1}^{2.5} Sv\,(\xi, T)\,\mathrm{dT}. \qquad (7)$$

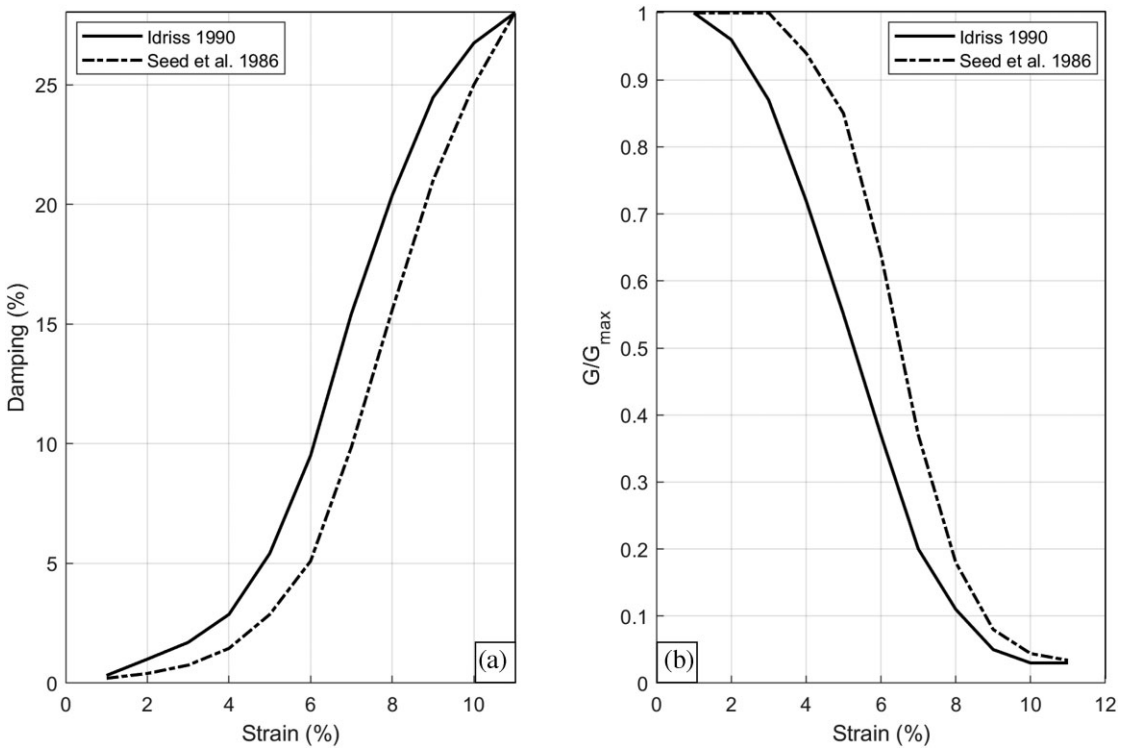

Figure 6. (a) Shear modulus and (b) damping curves adopted for 1D seismic site response of ZONE 1 (Idriss 1991) and ZONE 2 (Seed *et al.* 1986).

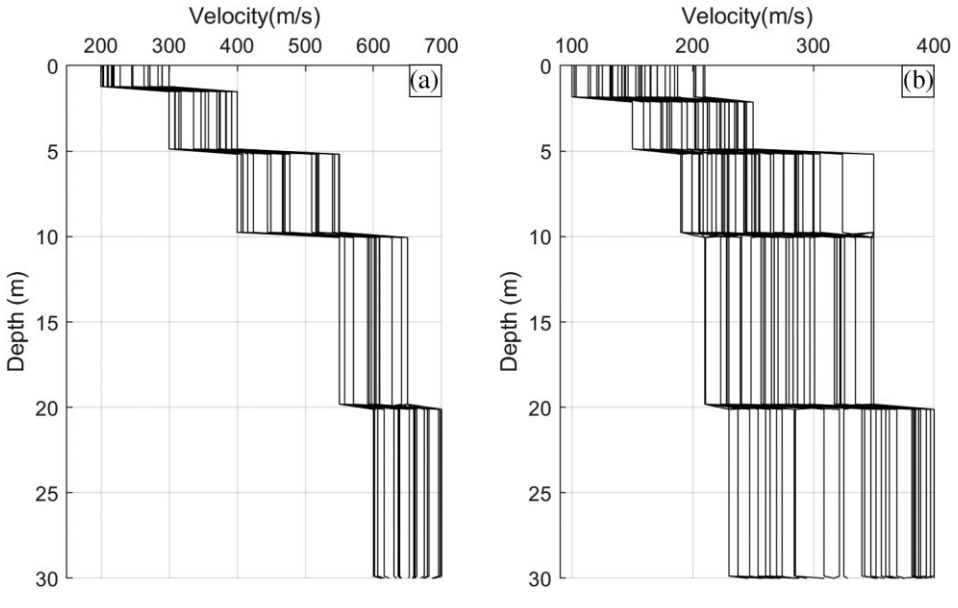

Figure 7. Example of 100 realisations of V_S profiles for (a) ZONE 1 and (b) ZONE 2.

The time integral considers the area under the pseudo-velocity response spectra S_v over the period range T between 0.1 and 2.5 s, with a damping ratio (ξ) of 5%. This is an important parameter (expressed in cm), commonly adopted to evaluate the seismic input energy and buildings damage capacity (Housner 1952).

STRATA software generates different outputs such as the acceleration time histories and the response spectra. The PGA and Housner Intensity are calculated a posteriori.

The resulting spectral acceleration curves for ZONES 1 and 2 are shown in figure 8 parts a and b, respectively. They are computed as the mean of all Monte Carlo simulations. Each curve is normalised to the common initial value of spectral acceleration, which is equal to 0.1 *g*. The response spectra obtained from the simulation of the velocity gradients of

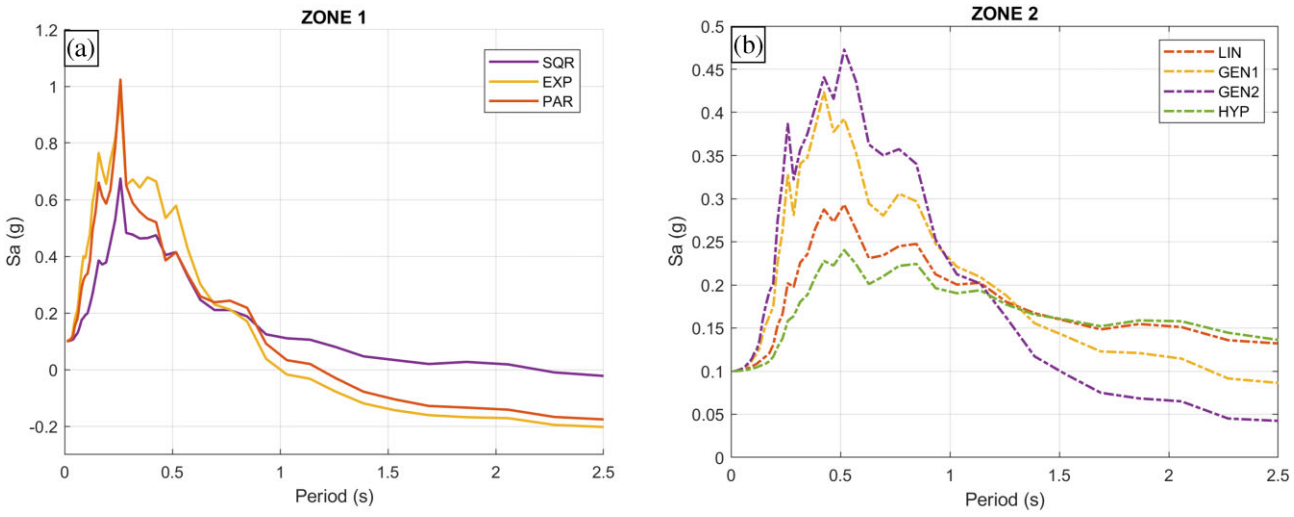

Figure 8. Mean response spectra at the ground surface for the different velocity gradients used to define the V_S profiles in (a) ZONE 1 and (b) ZONE 2.

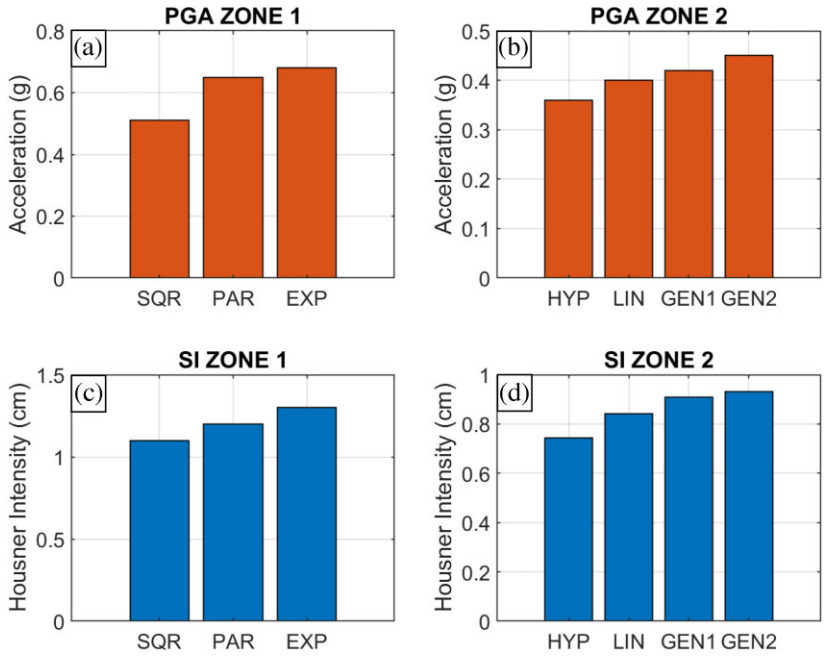

Figure 9. PGA (a, b) and Housner Spectrum Intensity SI (c, d) values, inferred from the simulations.

ZONES 1 and 2 show significant amplifications in the period range of engineering interest, with high amplifications at low periods. The peak value of spectral acceleration increases gradually from 0.64 *g* to 1.3 *g* for ZONE 1 and from 0.25 *g* to 0.48 *g* for ZONE 2**.**

It is possible to observe the same relative differences in PGA values (figure 9). In particular, the values of PGA span from 0.51 *g* to 0.68 *g* for ZONE 1 (figure 9a), and between 0.36 *g* and 0.45 *g* for ZONE 2 (figure 9b).

Figure 9 shows the Housner Spectrum Intensity values inferred from the spectra for each velocity gradient adopted in this study. The Housner Spectrum Intensities range between 1.1 and 1.3 cm for ZONE 1 (figure 9c), and between 0.74 and 0.93 cm for ZONE 2 (figure 9d).

5. Comparison with real accelerograms

In this section, we compare the results of 1D seismic site response and real data collected in Casaglia site where a borehole was available (see location in figure 2). The borehole is located in Po alluvial plain (the geological context called 'ZONE 2' in this study). The borehole reaches the Quaternary basement at 132 m deep. The sedimentary coverage is represented by Holocenic alluvial deposits, varying from clay

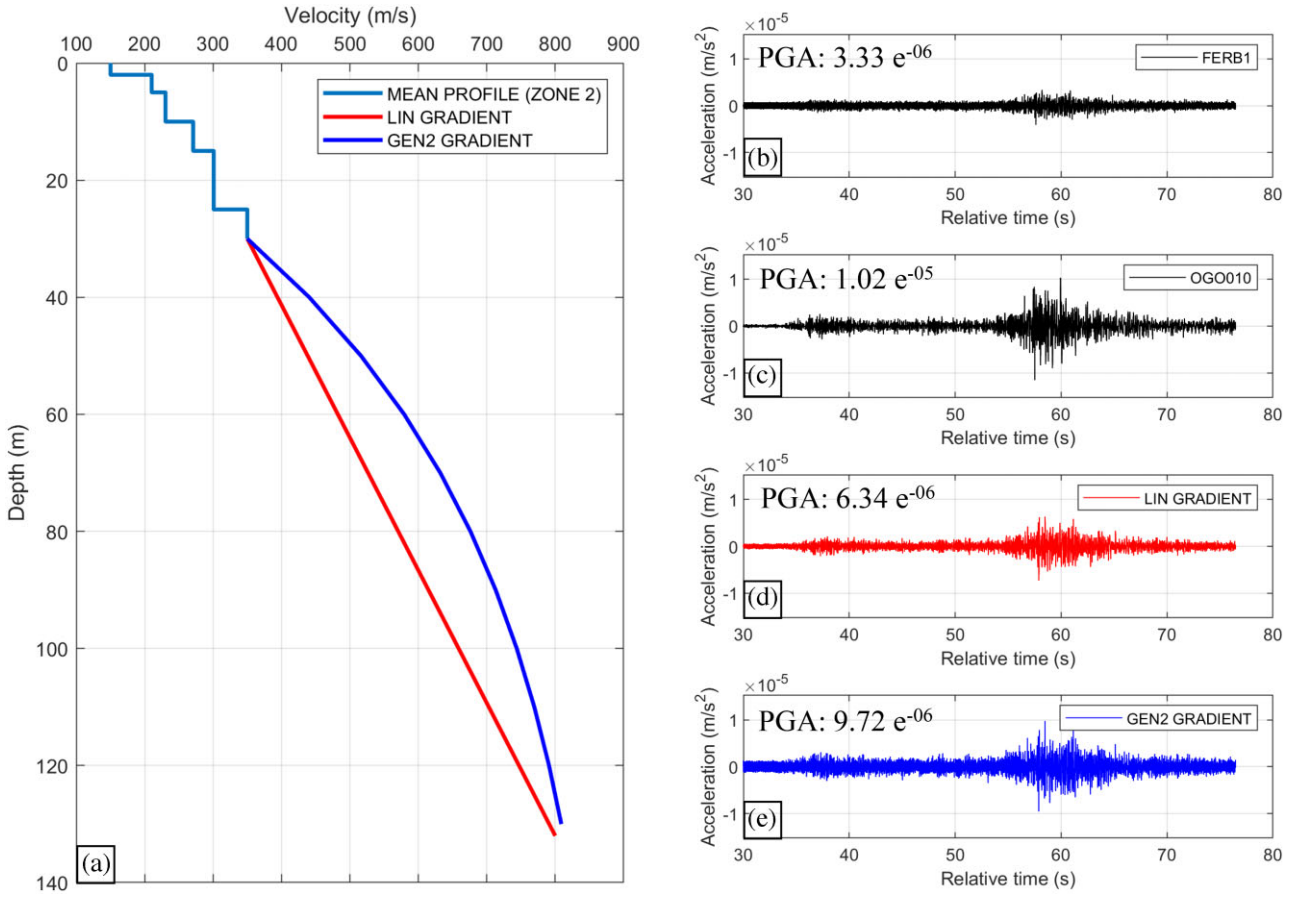

Figure 10. (a) Shear-wave velocity structures used as model for the alluvial sedimentary cover in Casaglia site (see figure 2). (b) Accelerogram of the seismic event occurred on 12 February 2013 recorded by the borehole seismic stations (FERB); (c) the same seismic event recorded by the surface station located at the top of the borehole (OG010); (d) simulated accelerogram inferred from a linear gradient LIN and (e) simulated accelerogram inferred from an exponential gradient GEN2.

to coarse loose sand poorly compacted. The site can be classified as soft soil, according to cross-hole and down-hole measurements by Pesaresi *et al.* (2014).

On the basis of this specific stratigraphic information until 132 m deep, we model the 1D shear-wave velocity structure. The first 30 m are modelled with the mean V_S profile that characterise ZONE 2 (figure 4). The engineering bedrock depth is assumed to be at 132 m, as suggested by the stratigraphic log, so the deeper velocity structures are extrapolated with LIN and GEN2 gradients (equations (4) and (6)). The V_S profiles adopted for seismic site response are shown in figure 10a.

The borehole was equipped with two broadband seismometers, one at the surface (OG010, a Lennartz velocimeter) and the other at a depth of 135 m, within the Quaternary basement (FERB, a Guralp CMG-3TB seismometer). The available recorded waveforms refer to an aseismic event that occurred on 12 February 2013, with $M_L = 3.8$ and an epicentral distance of 170 km (Pesaresi *et al.* 2014). The east-component waveforms (expressed in m s^{-1}) are converted in accelerograms and are shown in figure 10b and c, with their corresponding PGAs. It is worth noticing that the PGA recorded by the borehole station is smaller than the one recorded by the surface station, due to the soft layer amplification of motion.

To compare different *Vs* gradients, the waveform recorded by the borehole station was used as input motion for the 1D seismic site response computed with STRATA software. Figure 10c and d show the simulated accelerograms for the LIN and GEN2 gradients. The computed PGAs are also displayed. As expected, the linear gradient LIN (as suggested by the norms) underestimates the amplification effects, with a variation of the amplification effects of 43%. On the contrary, the synthetic accelerogram computed with the non-linear gradient GEN2 is characterised by a PGA value similar to the real ones recorded at the surface.

6. Discussions and conclusion

In this study, we compute the 1D seismic site response of two sectors of the Venetian Plain, where deep V_S profiles are

unknown, adopting several shear-wave velocity gradients found in literature. Our study demonstrates how the choice of the velocity gradient curves has a significant impact on the seismic site response in terms of PGAs, Spectral Accelerations and Housner Intensities. These three parameters are fundamental for strong ground motion prediction and they are the most adopted in engineering aseismic design. We consider two sectors of the Venetian Plain: ZONE 1 with gravel formations and an unknown bedrock depth and ZONE 2 with sandy-clay formations and a known bedrock depth.

In ZONE 1, where the bedrock depth is unknown, the choice of the velocity gradient determines the engineering bedrock depth, ranging between 60 and 180 m (figure 5a). In this case, the different results depend mainly on the variable thickness of the soft sedimentary layer, which is excited by the seismic input during the simulation. In particular, it is possible to observe a decrease in the amplification effects with the increase of the bedrock depth. The results related to the EXP gradient (equation (1)) present the highest amplifications, being in these terms the most conservative for the prediction of the seismic action (figures 8a and 9a,c).

In ZONE 2, where the bedrock depth is known, the soft soil column has a constant thickness of 400 m, but the shape of the velocity profiles between the 30 m and the engineering bedrock is significantly different (figure 5b). In this case, the stochastic simulation based on the use of different velocity gradients shows differences up to 20%. The smaller site response is associated to the LIN and HYP gradients (equations (4) and (7)), characterised by lower values of V_S, e.g. softer soils (figures 8b and 9b,d). The softer sites are able to accumulate larger strains and experience more damping. In particular, considering the case of a thick soil column, the damping is much more pronounced; thus, in this condition, the attenuation phenomena become dominant (Boaga *et al.* 2015).

Keeping a conservative approach for seismic design, it appears more appropriate to model the soil column with GEN1 or GEN2 gradients (equations (5) and (6)), which allow us to obtain the highest values of PGA, Spectral Acceleration and Housner Spectrum Intensity.

We evaluate the effect of the V_S gradient choice also considering real seismic data recorded at 135 m deep and at the surface in a borehole located in the Po Plain. In this way, we investigate the site amplification of the sedimentary columns between the down-hole and surface station, modelled with different types of gradients. The linear gradient method (as suggested by several seismic design norms) here again underestimates the seismic site amplification, while the non-linear gradient GEN2 reliably estimates the site amplification effect (figure 10a,d,e). This experimental study case confirms the importance of choosing an appropriate gradient in alluvial plains for an estimation of seismic effects. However, the only available accelerograms for the 1D seismic site response analysis of Casaglia site are characterised by small acceleration values, thus it could be difficult to establish the real implication for a structural aseismic design.

To avoid estimation errors induced by an arbitrary choice of the velocity gradient, the regional deep basin structure should be determined through deep geophysical investigations (e.g. seismic reflection surveys, passive surface wave techniques, etc.). When these seismic surveys are not logistically possible, it seems more appropriate to model the soil column with the V_S gradient which allows obtaining the most conservative approach, i.e. stronger seismic ground motion.

Acknowledgement

The authors thank Dr Damiano Pesaresi who provide the seismic data recorded at Casaglia site.

Author Contributions

All authors contributed to the study conception and design. Material preparation, data collection and analysis were performed by Valeria Cascone, Ilaria Barone and Jacopo Boaga. The first draft of the paper was written by Valeria Cascone and all authors commented on previous versions of the paper. All authors read and approved the final paper.

Conflict of interest statement. The authors declare no conflicts of interest.

References

Albarello, D., Cesi, C., Eulilli, V., Guerrini, F., Lunedei, E., Paolucci, E. & Puzzilli, L. M., 2011. The contribution of the ambient vibration prospecting in seismic microzoning: an example from the area damaged by the April 6, 2009 L'Aquila (Italy) earthquake, *Bollettino di Geofisica Teorica e Applicata*, **52**, 513–538.

Andreotti, G., Famà, A & Lai, C.G., 2018. Hazard-dependent soil factors for site-specific elastic acceleration response spectra of Italian and European seismic building codes, *Bulletin of Earthquake Engineering*, **16**, 5769–5800.

Barbellini, A., Morelli, A & Ferreira, A.M., 2017. Crustal structure of northern Italy from the ellipticity of Rayleigh waves, *Physics of the Earth and Planetary Interiors*, **265**, 1–14.

Boaga, J., 2013. An efficient tool for cultural heritage seismic soil classification: frequency-time analysis method in Venice historical center and its lagoon (Italy), *Geosciences Journal*, **17**, 301–311.

Boaga, J., Renzi, S., Deiana, R. & Cassiani, G., 2015. Soil damping influence on seismic ground response: a parametric analysis for weak to moderate ground motion, *Soil Dynamics and Earthquake Engineering*, **79**, 71–79.

Boaga, J., Vignoli, G. & Cassiani, G., 2012. Shear wave profile from surface wave inversion: the impact of uncertainty on seismic site response analysis, *Journal of Geophysics and Engineering*, **9**, 244–246.

Boore, D.M., Joyner, W.B. & Fumal, T. E., 1993. Estimation of response spectra and peak accelerations from western North American earthquakes. Technical report.

Borcherdt, R.D., 1994. Estimates of site-dependent response spectra for design (methodology and justification), *Earthquake spectra*, **10**, 617–653.

Budny, M., 1984: *Seismische Bestimmung der bodendynamischen Kennwerte von oberflächennahen Schichten in Erdbebengebieten der Niederrheinischen Bucht und ihre ingenieurseismologische Anwendung. PhD thesis*, Geologisches Institut der Universität zu Köln.

Building Seismic Safety Council-BSSC. 2003. NEHRP-recommended provisions for seismic regulations for new buildings and other structures, *Federal Emergency Management Agency- Fema*, **302**, 303.

Cardarelli, E., Cercato, M. & De Donno, G., 2018. Surface and borehole geophysics for the rehabilitation of a concrete dam (Penne, Central Italy), *Engineering Geology*, **241**, 1–10.

Carminati, E., Doglioni, C. & Scrocca, D., 2003. Apennines subduction-related subsidence of Venice (Italy), *Geophysical Research Letters*, **30**, 47–50**.**

Carraro, A., Fabbri, P., Giaretta, A., Peruzzo, L., Tateo, F. & Tellini, F., 2015. Effects of redox conditions on the control of arsenic mobility in shallow alluvial aquifers on the Venetian Plain (Italy), *Science of the Total Environment*, **532**, 581–594.

Cassinis, R., 2006. Reviewing pre-TRANSALP DSS models, *Tectonophysics*, **414**, 79–86.

Chong, J. & Ni, S., 2009. Near surface velocity and Q_S structure of the Quaternary sediment in Bohai basin, China, *Earthquake Science*, **22,** 451–458.

Claprood, M. & Asten, M.W, 2010. Statistical validity control on SPAC microtremor observations recorded with a restricted number of sensors, *Bulletin of the Seismological Society of America*, **100,** 776–791.

Doglioni, C., 1993. Some remarks on the origin of foredeeps, *Tectonophysics*, **228**, 1–20.

European Committee for Standardization, 2004. Eurocode 8: Design of structures for earthquake resistance, P1: General rules, seismic actions and rules for buildings, Draft 6, Doc CEN /TC250/SC8/N335.

Faccioli, E., Paolucci, R. & Vanini, M., 2015. Evaluation of probabilistic site-specific seismic-hazard methods and associated uncertainties, with applications in the Po Plain, northern Italy. *Bulletin of the Seismological Society of America*, **105**, 2787–2807.

Gibson, E., 1967. Some results concerning displacements and stresses in a non-homogeneous elastic half-space. *Geotechnique*, **17**, 58–67.

Gruppo di Lavoro, ICMS, 2018. Indirizzi e criteri per la microzonazione sismica. In *Conferenza delle Regioni e delle Provincie autonome. Dipartimento della protezione civile*, (Vol. 3) Roma.

Gruppo di Mappa di Pericolosità Sismica (GdL MPS), 2004. *Redazione della mappa di pericolosità sismica prevista dall'Ordinanza PCM 3274 del 20 marzo 2003, Rapporto conclusivo per il dipartimento di Protezione Civile*, INGV, Milano, Roma, 65 pp., available at http ://zonesismiche.mi.ingv.it

Guéguen, P., Cornou, C., Garambois, S. & Banton, J., 2007. On the limitation of the H/V spectral ratio using seismic noise as an exploration tool: application to the Grenoble valley (France), a small apex ratio basin. *Pure and Applied Geophysics*, **164**, 115–134.

Housner, G.W., 1952. *Intensity of Ground Motion during Strong Earthquakes*. California Institute of Tech Pasadena Earthquake Engineering Research Laboratory.

Hunter, J.A., Benjumea, B., Harris, J.B., Miller, R.D., Pullan, S.E., Burns, R.A. & Good, R.L, 2002. Surface and downhole shear wave seismic methods for thick soil site investigations, *Soil Dynamics and Earthquake Engineering*, **22**, 931–941.

Idriss, I., 1991. Earthquake Ground Motions at Soft Soil Sites. International Conferences on Recent Advances in Geotechnical Earthquake Engineering and Soil Dynamics. 3.

Idriss, I.M. & Sun, J.I., 1992. *SHAKE91: A Computer Program for Conducting Equivalent Linear Seismic Response Analyses of Horizontally Layered Soil Deposits*. Center for Geotechnical Modeling, Department of Civil and Environmental Engineering, University of California, Davis, CA.

Iervolino, I., Galasso, C. & Cosenza, E., 2009. REXEL: computer aided record selection for code-based seismic structural analysis. *Bulletin of Earthquake Engineering*, **8**, 339–362.

Kottke, A.R. & Rathje, E.M., 2009. *Technical Manual for Strata*. PEER Report, Pacific Earthquake Engineering Research Center

Kramer, S. L., 1996. *Geotechnical Earthquake Engineering*. Prentice Hall, Upper Saddle River, N.J

Lacoss, R.T., Kelly, E.J. & Toksöz, M.N., 1969. Estimation of seismic noise structure using arrays. *Geophysics*, **34**, 21–38.

Langston, C.A., 2003. Local earthquake wave propagation through Mississippi embayment sediments, part I: body-wave phases and local site responses. *Bulletin of the Seismological Society of America*; **93**, 2664–2684.

Louie, J.N., 2001. Faster, better: shear-wave velocity to 100 meters depth from refraction microtremor arrays. *Bulletin of the Seismological Society of America*, **91**, 347–364.

Martin, G.R. & Dobry,, R., 1994. Earthquake site response and seismic code provisions, *NCEER Bulletin*, **8.4**, 1–6.

Mascandola, C., Massa, M., Barani, S., Albarello, D., Lovati, S., Martelli, L. & Poggi, V., 2019. Mapping the seismic bedrock of the Po Plain (Italy) through ambient-vibration monitoring, *Bulletin of the Seismological Society of America*, **109**, 164–177.

Nakamura, Y., 1989. A method for dynamic characteristics estimation of sub-surface using microtremor on the ground surface, *Quarterly Report of Railway Technical Research Institute*, **30**, 25–33.

Norme Tecniche per le Costruzioni, 2008. Aggiornamento delle Norme tecniche per le costruzioni. *Gazzetta Ufficiale Serie Generale*.

Park, C.B., Miller, R.D., Xia, J., Ivanov, J., Hunter, J.A., Good, R.L. & Burns, R.A., 2000. Multichannel analysis of underwater surface waves near Vancouver, BC, Canada. In *SEG Technical Program Expanded Abstracts 2000*, pp. 1303–1306.

Pesaresi, D., Romanelli, M., Barnaba, C., Bragato, P.L. & Durì, G., 2014. OGS improvements in 2012 in running the North-eastern Italy seismic network: the Ferrara VBB borehole seismic station. *Advances in Geosciences*, **36**, 61–67.

Pitilakis, K., Alexoudi, M., Argyrodius, S. & Anastasiadis, A., 2006. Seismic risk scenarios for an efficient seismic risk management: the case of Thessaloniki (Greece). In *Advances in Earthquake Engineering for Urban Risk Reduction*, 229–244. Springer, Dordrecht.

Poggi, V., Fäh, D., Burjanek, J. & Giardini, D., 2012. The use of Rayleigh-wave ellipticity for site-specific hazard assessment and microzonation: application to the city of Lucerne, Switzerland, *Geophysical Journal. International* **188**, 1154–1172.

Poli, M.E., Burrato, P., Galadini, F. & Zanferrari, A., 2008. Seismogenic sources responsible for destructive earthquakes in north-eastern Italy. *Bollettino di Geofisica Teorica e Applicata*, **49**, 301–313.

Rathje, E.M., Kottke, A.R. & Trent, W.L, 2010. Influence of input motion and site property variabilities on seismic site response analysis. *Journal of geotechnical and geoenvironmental engineering*, **136**, 607–619.

Régnier, J., Bonilla, L.F., Bard, P.Y., Bertrand, E., Hollender, F., Kawase, H. & Boldini, D., 2016. International benchmark on numerical simulations for 1D, nonlinear site response (PRENOLIN): Verification phase based on canonical cases. *Bulletin of the Seismological Society of America*, **106**, 2112–2135.

Santamarina, J.C., Klein, K.A. & Fam, M.A., 2001. *Soils and Waves–Particulate Materials Behavior, Characterization and Process Monitoring*. Wiley, Chichester

Schnabel, P.B., Lysmer, J. & Seed, H.B., 1972. *SHAKE: A computer program for earthquake response analysis of horizontally layered sites*. Report No. EERC 72-12, Earthquake Engineering Research Center, University of California, Berkeley.

Seed, H.B., Wong, R.T., Idriss, I.M. & Tokimatsu, K., 1986. Moduli and damping factors for dynamic analyses of cohesionless soils. *Journal of Geotechnical Engineering*, **112**, 1016–1032.

Strobbia, C., Andreas, L., Vermeer, P. & Glushchenko, A., 2011. Surface waves: use them then lose them. Surface-wave analysis, inversion and attenuation in land reflection seismic surveying, *Near Surface Geophysics*, **9**, 503–513.

Strobbia, C., Boaga, J. & Cassiani, G., 2015. Double-array refraction microtremors. *Journal of Applied Geophysics*, **121**, 31–41.

TRANSALP Working Group, 2002. First deep seismic reflection images of the Eastern Alps reveal giant crustal wedges and transcrustal ramps, *Geophysical Research Letters*, **29**, doi: 10.1029/2002GL014911.

Vuan, A., Klin, P., Laurenzano, G. & Priolo, E., 2011. Far-source long-period displacement response spectra in the Po and Venetian Plains (Italy) from 3D wavefield simulations. *Bulletin of the Seismological Society of America*, **101**, 1055–1072.